# Evaluating the real changes of air quality due to clean air actions using a machine learning technique

Guo, Yong; Li, Kangwei; Zhao, Bin; Shen, Jiandong; Bloss, William J.; Azzi, Merched; Zhang, Yinping

*DOI:*
10.1016/j.chemosphere.2022.134608

# Evaluating the real changes of air quality due to clean air actions using a machine learning technique: results from 12 Chinese mega-cities during 2013-2020

Yong Guo[1,2], Kangwei Li[3*], Bin Zhao[4], Jiandong Shen[5], William J. Bloss[6], Merched Azzi[7], Yinping Zhang[1,2]

*[1]Department of Building Science, Tsinghua University, Beijing, China*
*[2]Beijing Key Laboratory of Indoor Air Quality Evaluation and Control, Beijing, China*
*[3]Univ Lyon, Université Claude Bernard Lyon 1, CNRS, IRCELYON, F-69626 Villeurbanne, France*
*[4] School of Environment, and State Key Joint Laboratory of Environment Simulation and Pollution Control, Tsinghua University, Beijing 100084, China*
*[5] Hangzhou Environmental Monitoring Center Station, Hangzhou 310007, China*
*[6] School of Geography, Earth and Environmental Sciences, University of Birmingham, Birmingham, United Kingdom*
*[7] New South Wales Department of Planning, Industry and Environment, PO Box 29, Lidcombe, NSW 1825, Australia*

***Corresponding to Kangwei Li (likangweizju@foxmail.com ; kangwei.li@ircelyon.univ-lyon1.fr)**

## Abstract

China has implemented two national clean air actions in 2013-2017 and 2018-2020, respectively, with the aim of reducing primary emissions and hence improving air quality at a national level. It is important to examine the effectiveness of such emission reductions and assess the resulting changes in air quality. However, such evaluation is difficult as meteorological factors can amplify, or obscure the changes of air pollutants, in addition to the emission reduction. In this study, we applied the random forest machine learning technique to decouple meteorological influences from emissions changes, and examined the deweathered trends of air pollutants in 12 Chinese mega-cities during 2013-2020. The observed concentrations of all criteria pollutants except $O_3$ showed significant declines from 2013 to 2020, with $PM_{2.5}$ annual decline rates of 6-9% in most cities. In contrast, $O_3$ concentrations increased with annual growth rates of 1-9%. Compared with the observed results, all the pollutants showed smoothed but similar variation in trend and annual rate-of-change after weather normalization. The response of $O_3$ to $NO_2$ concentrations indicated significant regional differences in photochemical regimes, and the differences between observed and deweathered results provided implications for volatile organic compound emission reductions in $O_3$ pollution mitigation. We further evaluated the effectiveness of first and second clean air actions by removing the meteorological influence. We found that the meteorology can make negative or positive contribution in reducing pollutant concentrations from emission reduction, depending on type of pollutants, locations, and time period. Among the 12 mega-cities, only Beijing showed a positive meteorological contribution in amplifying reductions in main pollutants except $O_3$ during both clean air action periods. Considering the large and variable impact of meteorological effects in changing air quality, we suggest that similar deweathered analysis is needed as a routine policy evaluation tool on a regional basis.

**Keywords**: air quality, clean air action, weather normalization, random forest model, meteorological influence

**Graphical Abstract**

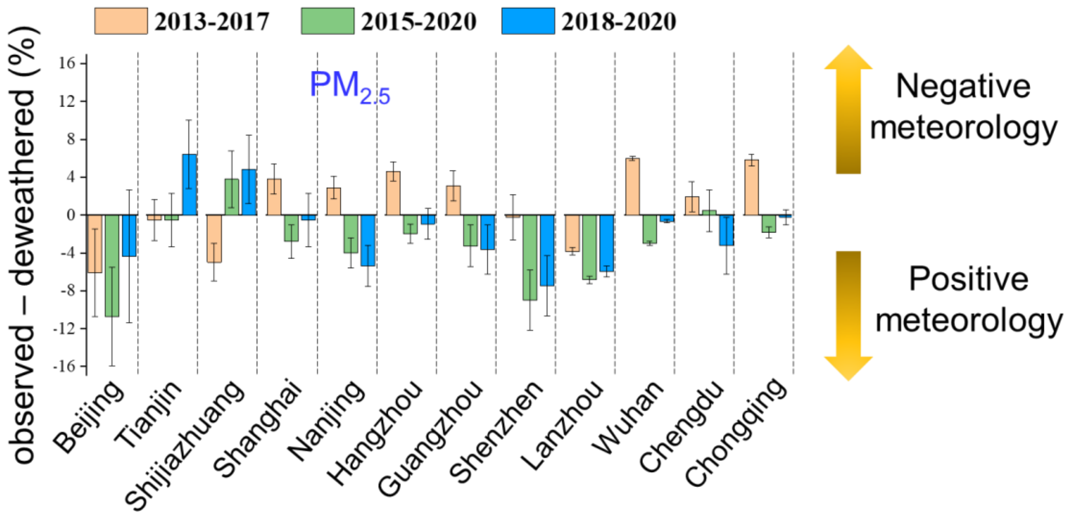


## 1. Introduction

Air pollution is an urgent problem globally due to its adverse impacts on the environment, human health and climate (Fan et al., 2020; Hadley et al., 2018). It has been well recognized $SO_2$, $NO_2$, CO, $O_3$, $PM_{2.5}$ and $PM_{10}$ are defined as the six criteria pollutants in quantifying air pollution levels (Hu et al., 2015). World Health Organization (WHO) data shows that 9 out of 10 people breathe air that contains high levels of these criteria pollutants and which exceeds WHO guideline limits, and it is estimated that 7 million people premature deaths are caused by air pollution worldwide every year (World Health Organization, 2021). In addition, air pollution can reduce visibility and affect solar radiation balance directly and indirectly (Li. et al., 2017; Xia et al., 2016), and even give rise to more extreme weather events (i.e. flooding and drought (Cui et al., 2017; Herrera-Estrada et al., 2018; Tie et al., 2016).

In the past few decades, China has experienced rapid industrialization and urbanization. Along with the rapid development of the economy, air pollution has produced a substantial influence on each sector of Chinese society for a long time. In some major areas of China, concentrations of air pollutants greatly exceed air quality guidelines for the protection of health recommended by the WHO (Zhang et al., 2015). In China, ambient air pollution has become the fourth largest threat to Chinese health, after heart disease, dietary risks and smoking (Chen et al., 2013; Zhang et al., 2015), and was responsible for 1,565,000 to 2,168,000 premature deaths in 2019 (http://ghdx.healthdata.org/gbd-results-tool). As a result, air pollution has become a major concern for the public and policy makers (Feng et al., 2017; Guo et al., 2020; Kuerban et al., 2020; Liu and Wang, 2020; Ma et al., 2019; Song et al., 2017; Wang et al., 2019a; Wang et al., 2019b; Zhan et al., 2018; Zhang et al., 2018). To solve the increasingly serious air pollution problem, China established a national air quality monitoring network that covers major cities since early 2013. The monitoring data include observations of $PM_{2.5}$, $PM_{10}$, $NO_2$, $SO_2$, $O_3$ and CO (Wang et al., 2020b). Meanwhile in 2013, the Chinese government implemented the "Air Pollution Prevention and Control Action Plan" (2013-2017), also known as the first Clean Air Action. In 2018, the Chinese government continued to implement the "Blue Sky Protection Campaign" (2018-2020), also known as the second Clean Air Action (Wang et al., 2019c; Xu et al., 2021).

At present, these actions have been implemented, and it is of great significance to accurately estimate whether the intervention is working to meet the set targets. However, such evaluation is somewhat difficult as many meteorological conditions can obscure the impact of emission changes on air quality (Vu et al., 2019). Apart from interventions or management efforts to control air pollution, meteorological conditions can also directly or indirectly affect the emission, transport, chemical formation and deposition of air pollutants, thus affecting their concentration in ambient air (Zhang et al., 2015). Variation of meteorological factors can hinder the correct analysis of trends in different air pollutants and may lead to erroneous conclusions about the effectiveness of intervention or management strategies (Grange and Carslaw, 2019). Hence, it is essential to decouple meteorological impacts from trends in ambient air quality data and extract the real changes in air quality driven by policy interventions.

Daskalakis et al. (2016) employed chemical transport models to evaluate the response of air quality to emission control measures, which was based on assimilated meteorology to account for the year-to-year climate variability. However, such assessment results will be affected by significant uncertainties in the emission inventory and chemical transport model itself (Gao et al., 2018). Statistical analysis is another commonly used method to decouple the meteorological effects on air quality. Many mathematical analysis approaches or models were developed, which were mainly through data regression to eliminate the impact of varying meteorological variables. Venter et al. (2020) adopted a regression model to evaluate the effects of COVID-19 lockdown on air pollution levels. He et al. (2020) applied a “difference-in-difference” approach to evaluate the impacts of COVID-19 lockdown measures in terms of the Air Quality Index (AQI) and the concentrations of particulate matter. Henneman et al. (2015) employed multiple Kolmogorov–Zurbenko filters and a multi-linear regression model to estimate the effectiveness of air pollution regulations and control measures. Among these models, machine learning models (i.e., the boosted regression trees and random forest algorithms) usually show a better performance than traditional statistical and air quality models by reducing variance/bias and error in high dimensional data sets, though they fail to interpret the physical mechanism behind the results (Zhang et al., 2020). Particularly, RF has the advantage of not being a "black-box" method where the learning process can be explained, investigated, and interpreted. Recently, Grange et al. (2018) developed a machine learning technique based upon the random forest algorithm to identify the key mitigation measures contributing to the reduction of air pollutant concentrations in Beijing. This technique has been adopted widely and validated in various environments (Shi et al., 2021; Vu et al., 2019; Zhang et al., 2020).

In this study, we applied the RF machine learning technique proposed by Vu et al. (2019), and systematically studied the trends and characteristics of air pollution in 12 mega-cities in China from 2013 to 2020 based on the latest observational data. The effects of meteorological factors were eliminated from the trends in pollutant levels, and the real performance of the two national clean air actions were comprehensively assessed. The results may be conducive to formulating air quality control policies in China and other developing countries.

# 2. Method

2.1 Study region and data sources

In this study, we investigated 12 megacities in China, these cities are selected as they are representative mega-cities of China according to their GDP, population and area, and geographical distribution. Also, the air quality data availability is another important reason, as all these 12 mega-cities started to monitor $PM_{2.5}$ since January 2013. Their geographical locations are shown in Fig. S1, and the summarized information describing each city (i.e. economy, population, area, specific location, etc.) can be found in the Supporting Information Table S1.

Since January 2013, the Ministry of Environmental Protection of China (MEPC) has released the real-time air pollution monitoring information for 74 major cities, including for the 6 main criteria pollutants of $PM_{2.5}$, $PM_{10}$, $NO_2$, $SO_2$, $O_3$ and CO. In this study, we used air quality observation data and meteorological data over the aforementioned 12 cities from 18th January 2013 to 31st December 2020. Table S2 summarized the name and location of monitoring stations in each city from the Chinese national monitoring network, and those sites are mostly distributed in urban areas of each city. By averaging the measurements from the monitoring sites within each city, we obtain city-specific dataset that can represent the air quality of each city. Meteorological data, including air pressure (PRS, hPa), temperature (TMP, °C), wind direction (WD, °), wind speed (WS, m/s), and humidity (RH, %), were also collected from meteorological stations of each city over the period of 18th January 2013 to 31st December 2020. The detailed information of data source was illustrated in Supporting Information Text S1.

2.2 Deweathering using the random forest (RF) model

The deweathering technique was first proposed by Grange et al. (2018) to predict the concentrations of air pollutants at a specific measured time point but removing the influence of varying meteorological conditions, which was regarded as "deweathered concentration". Such technique was based on RF regression model. Regression model is a mathematical model for quantitative description of statistical relationship, and it can indicate the strength of the influence of multiple independent variables on one dependent variable. The RF regression model is composed of hundreds of independent decision tree models and a combination of randomly chosen explanatory factors, and the term "Random Forests" is derived from "random decision forests". The random selection process involves 1) variables and data input, and 2) generation of a certain number of decision trees. In the subsequent calculation, each decision tree can provide one intermediate for the input variables, and then the intermediate of these decision trees were summarized as the RF regression prediction result. It can be employed to describe the relationship between the concentration of air pollutants by temporal variables (yearly, day of year, day of week, and hourly) and meteorological variables (relative humidity, temperature, atmospheric pressure, wind speed and wind direction). The detailed information of random forest model can be found in Supporting Information Text S2 (Wang et al., 2020a).

Firstly, we constructed a reliable RF model. The original datasets for the RF model of each city contain the concentration of $PM_{2.5}$, $PM_{10}$, $NO_2$, $SO_2$, $O_3$ and CO as well as their predictor variables, including time variables represented by Unix Epoch time, hour (0−23), day of week (Monday to Sunday), and meteorological parameters (wind speed, wind direction, pressure, temperature, and RH). 70% of the original datasets were randomly selected as a training dataset to construct the RF model, using R “normalweather” packages by Grange et al. (2018), and the remaining 30% of the original data was employed as testing dataset to validate the performance of the constructed model. The performance of the RF model has been evaluated based on several typical statistical metrics (Emery et al., 2017; Vu et al., 2019), and details of formulas, verification plots and summarized statistical metrics can be found in the Supporting Information Text S3, Fig. S3 and Table S3. These results demonstrated the reliability of the trained model. For example, the coefficient of determination $r^2$ are all above 0.8, and the coefficient of efficiency COE are between 0.6 and 0.9. These validation results from different statistical metrics are overall consistent with previous study (Vu et al., 2019), hence the trained model can be used for subsequent deweathering analysis.

Secondly, we used the validated RF model to eliminate the effects of meteorological factors. Both time variables (month, week, and hour) and meteorological parameters were resampled randomly to represent the mean meteorological conditions of a city. Specifically, we resampled meteorological data set from the meteorological conditions of that city for 2013-2020. The input meteorological variables at a particular time point on a particular day can be randomly replaced with data at the same time within a four-week period (i.e., 2 weeks before and 2 weeks after the selected date), which is similar to Zhang et al. (2020). Then the resampled meteorological variables and time variables were fed into the RF model to predict the concentrations of air pollutants. A diagram that describing the above methodology is shown in Fig. S2. This resample and calculation process was repeated 1000 times, and the 1000 predicted concentrations of each air pollutant at specific time point were obtained and then averaged as the final weather-normalized concentration. In this way, the impact of weather variations on air pollutants can be normalized while their seasonal and diurnal variations are retained, which allows us to further study the temporal variations in deweathered concentrations.

# 3. Results and discussion

## 3.1 Observed and deweathered air quality trends during 2013-2020

Combining the observed and deweathered pollution concentration data, we obtained the annual changing rate (normalized to the year of 2013) of the six criteria pollutants in the 12 mega-cities from 2013 to 2020 by a linear regression, which are shown in Fig. 1. Detailed trends about the monthly and yearly averaged values for both observed and deweathered concentrations can be found in Supporting Information Fig. S4-S5.

As shown in Fig. 1, the overall concentrations of $PM_{2.5}$ observed in 12 mega-cities maintained a general downward trend, while several cities experienced an uptick in specific years, such as Shijiazhuang in 2016 and Shanghai in 2015. Specifically, the annual decline rate of $PM_{2.5}$ observed across the 12 mega-cities has been around 6~9% per year, and the decline rates in Beijing, Shijiazhuang, Nanjing and Hangzhou are larger than for the other cities. The trends in the weather normalized concentrations and annual decline rates of $PM_{2.5}$ in most of the mega-cities are very similar to that of observed trends and annual decline rate, with the exceptions of Beijing and Lanzhou with 2% lower deweathered annual decline rate compared to that of observed $PM_{2.5}$.

Apart from Shijiazhuang, Lanzhou and Chengdu, the concentration of observed $PM_{10}$ in many cities increased in 2014 and then declined subsequently. The concentrations of observed $PM_{10}$ in Shijiazhuang, Lanzhou and Chengdu increased slightly in 2016 and maintained a downward trend in the other years. The annual decline rates of observed $PM_{10}$ are around 6%~8% in Beijing, Tianjin, Shijiazhuang, Nanjing, Wuhan, Chengdu and Chongqing, and 4%~6% in Shanghai, Hangzhou, Guangzhou, Shenzhen and Lanzhou. After weather normalization, the deweathered $PM_{10}$ showed overall similar annual decline rates to the observed, consistent with the case of $PM_{2.5}$.

Large variability in the trends for observed $NO_2$ concentrations were found among the 12 cities. Specifically, Chongqing and Lanzhou maintained an upward trend from 2013 to 2017, and began to decline from 2018. By contrast, other cities showed a downward trend of observed $NO_2$ since 2013 or 2014 with some fluctuations in specific years. In 2014, Tianjin, Shanghai, Lanzhou and Chongqing experienced a significant $NO_2$ uptick, while Nanjing, Hangzhou, Chengdu and Beijing experienced a sightly increase. In 2017, Tianjin, Guangzhou and Wuhan experienced a significant uptick while Nanjing and Shanghai experienced a sightly increase. Overall, the annual rate of decline of the observed $NO_2$ is highest in Beijing (7% per year), followed by Chengdu, Shenzhen and Wuhan (around 4%~6%), and the rates of decline for other cities are all below 4%. Comparatively, large fluctuations of the observed $NO_2$ in specific years were smoothed after the weather normalization. For example, the $NO_2$ increase phenomenon (i.e. Hangzhou and Chengdu in 2014; Tianjin and Guangzhou in 2017) was not observed in deweathered trends. The annual decline rates of $NO_2$ after the weather normalization were overall similar to that of the raw observed concentrations, except for Shanghai showing a clear difference between observed and deweathered (-0.4% vs. -2.1%).

The concentration of observed $O_3$ in most of the mega-cities showed an upward trend until 2017, except for Tianjin and Shijiazhuang. Specifically, Lanzhou, Shijiazhuang and Tianjin showed the highest annual rate of increase in observed $O_3$ at around 8%, followed by Nanjing (6%), while other cities showed lower rates of increase (below 4%). Similar to $NO_2$, the observed $O_3$ fluctuations in specific years were smoothed after the weather normalization. Overall, both observed and deweathered $O_3$ concentrations have increased for all the cities, with annual increase rates of 1- 9%.

The reduction in observed $SO_2$ concentrations was the most significant among the six criteria pollutants. From 2013 to 2020, all 12 mega-cities maintained a large $SO_2$ reduction rate in the first few years, which then gradually reduced. Particularly for Wuhan, Chongqing, Shenzhen, Lanzhou and Hangzhou, the observed $SO_2$ concentrations tended to flatten out since 2016. Overall, the annual rates of decline of observed $SO_2$ in most of the mega-cities exceeded 10%, with Beijing, Tianjin and Shijiazhuang showing the largest rate of decline (around 12%), while the rate of decline for Shenzhen is the lowest (6%). Compared to the observed results, almost all the mega-cities showed a similar trend and rate of decline in deweathered $SO_2$ results, except Lanzhou with a smaller decrease of deweathered trend than that observed since 2019.

Generally, the concentration of observed CO in all mega-cities showed a trend of declining concentrations, with some fluctuations for specific years. For example, Lanzhou and Chongqing showed a brief increase in observed CO in 2014, while Nanjing and Shijiazhuang also showed a significant increase of CO in 2016. Overall, Beijing, Tianjin, Shijiazhuang, Shenzhen and Chengdu showed a relatively large CO annual reduction rate of 6%~8%, while the reduction rate for other cities was around 2%~4%. Similar to other pollutants, the fluctuations of CO in specific years were smoothed after the weather normalization (i.e., Lanzhou and Chongqing in 2014; Nanjing in 2016). The annual rate of decline of CO after the weather normalization is very similar to that obtained from the observed values, with differences generally within 1%.

We further define the index $\omega$ to quantify the extent to which concentrations of the six criteria pollutants in different regions are affected by meteorological conditions. As meteorology may have positive or negative influences in different seasons (Vu et al., 2019), we used absolute difference between observed and deweathered values to prevent an offsetting effect arising between different seasons. The absolute difference values from 96 months between 2013 and 2020 are averaged, as shown in Equation (1).

$$\omega = \frac{\sum_{i=1}^{96} \frac{\left| C_{i,observation} - C_{i,model} \right|}{C_{i,observation}}}{96} \tag{1}$$

The $\omega$ values for the six criteria pollutants across 12 mega-cities are shown in Fig. S6 and the overall results are discussed here. $PM_{2.5}$, $PM_{10}$ and $O_3$ were most affected by meteorological conditions ($\omega$ between 10%~15%), followed by $NO_2$ and $SO_2$ ($\omega$ ~10%). Compared with other primary gaseous pollutants, it seems that $PM_{2.5}$ and $PM_{10}$ are more sensitive to meteorological influences. The likely reasons are 1) long-range transport is important source of aerosol, which is mainly controlled by the wind field; 2) temperature and humidity are also important meteorological factors that can affect secondary aerosol formation and chemical composition. CO shows the lowest $\omega$ value of around 5%, which may be explained by its long atmospheric lifetime that has least influence from meteorological conditions. Among 12 mega-cities, the air pollutants (i.e., $PM_{2.5}$, $PM_{10}$, $SO_2$ and CO) in Beijing are most affected by meteorological conditions, which is likely partly due to the unique topography in Beijing as the Yanshan Mountains and Taihang Mountains surround the city to the north and west. For example, northern winds tend to bring clean air to Beijing while southerly winds do the opposite (Liang et al., 2017; Zhang et al., 2015). Here we further performed the 72 hours backward trajectory analysis at Beijing from 2013 to 2020 by employing the hybrid single particle Lagrangian integrated trajectory model (Hysplit) with the global data assimilation system (GDAS). The trajectory clustering analysis showed that more than 50% long-range airmass arriving in Beijing were mainly originated from the northwest direction and passing through Yanshan Mountains and Taihang Mountains (Fig. S7). As mentioned previously, our RF model results suggested that Beijing is most affected by meteorological conditions among the 12 mega-cities, which may be explained by both unique topography in Beijing and frequent long-range airmass from northwest direction. By contrast, there were no significant city-to-city differences in the relative sensitivity to meteorological conditions for $NO_2$ and $O_3$.

## 3.2 Response of $O_3$ to $NO_2$ concentrations

It is well established that both NOx and volatile organic compounds (VOCs) are the precursors of $O_3$, and understanding the $O_3$-precursor relationship is important for developing effective $O_3$ control strategies (Blanchard, 2000; Hidy, 2000; Li et al., 2019; Lu et al., 2018). Here we explore the $O_3$-NOx relationship for each city by analysis of the monthly averaged $O_3$ and $NO_2$ concentrations (as volume mixing ratios, i.e. converted to ppbv to retain the $NO_2$-$O_3$ photostationary steady state stoichiometry) across all 96 months during 2013-2020 (Fig. 2). Data for most of the cities (except Guangzhou and Shenzhen) showed clear negative correlation between $O_3$ and $NO_2$, suggesting that NOx reduction can lead to the increase of $O_3$. According to the well-known titration reaction ($NO + O_3 \rightarrow NO_2 + O_2$), neglecting other processes an increase of 1 ppbv $NO_2$ would lead to 1 ppbv consumption of $O_3$, corresponding to a slope of $-1$ in the $O_3$ vs. $NO_2$ space. However, this slope value may vary due to the complex non-linearity of the $O_3$-VOC-NOx chemistry, which provides an indicator of the $O_3$ formation chemistry (i.e., $O_3$ formation is more or less sensitive to NOx reduction).

As shown in Fig. 2, the regression slope indicates how $O_3$ responses to the changes of NOx concentration for each city. Interestingly, it can be seen from observed category that the slope values showed significant regional differences with variations between cities. For example, the slope values for BTH region (Beijing-Tianjin-Hebei, Shijiazhuang is the capital of Hebei province) ranged from -1.42 to -1.36, while YRD region (Yangtze River Delta, including Shanghai, Hangzhou and Nanjing) ranged from -1.09 to -0.08. By contrast, data from the PRD region (Pearl River Delta, including Guangzhou and Shenzhen) did not show any clear negative relationship between $O_3$ and $NO_2$ (with slope of ~0). The above information is indicative of regional differences in $O_3$-precursor relationship. Here we further assume that the slope value of -1 as the threshold, with values significantly above or less than -1 as more or less sensitive to NOx reduction respectively. In addition, we compare our fitted slope values in $O_3$-$NO_2$ space with the $O_3$ formation regime identified from HCHO/$NO_2$ ratios in Li et al. (2021) for the three key regions. As shown in Table S4, these results are overall consistent, which further demonstrates that $O_3$ formation in PRD is more sensitive to NOx reduction, while $O_3$ formation in other regions is less sensitive to NOx reduction. Note that the above $O_3$-precursor relationship derived from the fitted slope value in the $O_3$ vs. $NO_2$ space is qualitative as a relative concept, and further detailed evaluation using a quantitative method (e.g. chemical transport model) is still needed.

Compared with the observed concentrations, the overall range in deweathered concentrations for $O_3$ and $NO_2$ are narrowed, suggesting that extreme conditions due to meteorology have been removed. Note that almost all the cities showed slightly decreased slopes ($O_3$ vs NOx) with improved $R^2$ after weather normalization, which implies a trend of $O_3$-precursor relationship towards less NOx sensitive condition. This suggests that using deweathered data more clearly demonstrates the need for VOC reductions – and the limitations of NOx-reductions alone – in reducing regional $O_3$ concentrations. The detailed reason for this phenomenon is unclear. However, it implies that the VOC emission reduction should play a more important role for $O_3$ pollution mitigation in most cities if the meteorological influence is considered.

## 3.3 Evaluating the effectiveness of two national clean air actions

### 3.3.1 First clean air action (2013-2017)

A series of policy, control measures and action plans were proposed for the first clean air action, with a particular focus on Beijing–Tianjin–Hebei, Yangtze River Delta, and Pearl River Delta regions, attempting to reduce $PM_{2.5}$ by 25%, 20%, and 15%, respectively. Table S5 summarized the main mitigation measures that implemented in China and other key regions during the clean air actions (Zhang et al., 2019; Zheng et al., 2018). Generally, these measures are overall similar among different regions, while there are some region-specific measures according to the differences in energy utilization and industry distribution for each region. According to the recent emission inventory (Zhang et al., 2019), China's anthropogenic emissions have been decreased by 59% for $SO_2$, 21% for NOx, 23% for CO, 36% for $PM_{10}$, and 33% for $PM_{2.5}$ during 2013–2017. To evaluate the effectiveness of the first clean air action, we summarized the results from the 12 mega-cities as derived from observations before and after weather normalization, as shown in Fig. S8 and Table 1.

It is evident that the first clean air action period shows significant reductions in $PM_{2.5}$ concentration, with both observed and deweathered $PM_{2.5}$ concentrations reducing by 34% on average the 12 mega-cities. The reductions indicated the effectiveness of mitigation efforts, such as strengthening industrial emission standards and replacing residential coal with electricity and natural gas (Zheng et al., 2018). The reduction percentages of $PM_{2.5}$ in Beijing and Shijiazhuang reduced greatly after weather normalization, suggesting that meteorological conditions made a positive and significant contribution in reducing $PM_{2.5}$ in Beijing and Shijiazhuang over this time period (see Table 1), while anthropogenic effects (i.e. impacts of emissions) did not reduce as much as the observations suggested (Li et al., 2020). In contrast, meteorological conditions made a negative contribution in suppressing reductions in $PM_{2.5}$ in Shanghai, Hangzhou, Wuhan and Chengdu, as the magnitudes of reduction increased after weather normalization, which is consistent with the conclusion of Xiao et al. (2021).

Although all the 12 mega-cities showed a downward trend in observed $PM_{10}$ from 2013 to 2017, the magnitudes of the reduction varied widely (0.8%~45%) among different cities and were lower than $PM_{2.5}$ in average (25% vs. 34%). This may partly be attributed to the greater importance of natural primary emission sources to $PM_{10}$, including dust storms from the desert areas in north and northwest of China (Li et al., 2017). The rates of reduction in deweathered $PM_{10}$ in Tianjin, Guangzhou, Wuhan and Chongqing were larger than the observed, while Beijing and Lanzhou showed the opposite characteristic. This indicates that the meteorological conditions made a negative contribution in suppressing reductions in $PM_{10}$ in Tianjin, Guangzhou, Wuhan and Chongqing, and a positive contribution in amplifying reductions in Beijing and Lanzhou. In general, the influences on $PM_{10}$ from meteorological conditions are limited compared with anthropogenic emission reduction.

$SO_2$ is mainly emitted from the coal-fired source, and the reductions in $SO_2$ concentration are in line with the coal-fired emission control measures (Li et al., 2020). All the 12 cities showed an obvious reduction in observed $SO_2$ from 2013 to 2017, which suggests that a remarkable $SO_2$ emission reduction was achieved in the first clean air action period, as all the 12 cities showed an obvious reduction in observed $SO_2$ from 2013 to 2017, and this is mainly due to the policy measures in phasing out of coal-fired boilers (Zheng et al., 2018). The reduction magnitudes of the observed $SO_2$ ranged from 27% (Shenzhen) to 70% (Beijing), with an average of 56%. All the 12 mega-cities showed very similar values (difference within 4%; see Table 1 and Fig. 3) between deweathered and observed $SO_2$ reduction magnitudes over 2013-2017, which implies that the meteorological effects can be negligible in obscuring changes in $SO_2$.

Some cities (e.g. Tianjin, Shanghai, Guangzhou, Lanzhou and Chongqing) showed 2.7%~47% increases in observed $NO_2$ from 2013 to 2017, while other cities showed 8.2%~18% reductions in the same period. The increase in observed $NO_2$ in some cities is mainly due to the increased vehicle emissions, as indicated by the rapid increase of car ownership in recent years (Song et al., 2018). After weather normalization, the increases in $NO_2$ in some cities (i.e. Tianjin, Shanghai and Lanzhou) were weakened and even reversed to become decreases (i.e. Guangzhou), while the magnitude of $NO_2$ reduction in Nanjing and Wuhan were enlarged. This suggests that the meteorological conditions made a negative contribution in obscuring $NO_2$ reductions in these cities. The effectiveness in reducing deweathered $NO_2$ was inferior to that of $SO_2$, which implies that the NOx from vehicle emissions were not as effectively controlled, as NOx emissions were from both coal-fired power plants and vehicle sources (Meng et al., 2018). Therefore, more effective control measures on vehicle emissions are needed (Lin et al., 2021).

As for $O_3$, most of the mega-cities (10 out of 12, except Guangzhou and Wuhan) showed an increase of observed $O_3$ from 2013 to 2017 with a range from 14% to 60%. After the weather normalization, the increase magnitudes of $O_3$ in Beijing, Tianjin and Shijiazhuang were lowered, suggesting that the increase of observed $O_3$ in these cities was partly due to the negative contribution of meteorological influence. As many previous studies have suggested that VOC-limited $O_3$ formation regimes dominate the urban areas of China (Ding et al., 2013), the decline in the NOx emission during the first clean air action can be regarded as a significant contributor to increasing $O_3$ concentration (Lin et al., 2021; Sun et al., 2019). Therefore, we believe that meteorology played an important but not dominant role in increasing the observed $O_3$ concentrations, consistent with previous studies (Chen et al., 2020a).

Most of the mega-cities (8 out of 12) showed 2.6%~31% reductions in observed CO from 2013 to 2017. By contrast, Shanghai, Nanjing, Lanzhou and Chongqing showed increases in observed CO from 1.6% to 29%. After weather normalization, the increases in CO were significantly weakened (i.e. Lanzhou) or even reversed (i.e. Shanghai and Nanjing). This suggests that meteorological conditions made a negative contribution in obscuring CO reductions in these cities. In general, the effectiveness in reducing CO varied in different cities, demonstrating that policy effectiveness in some cities (i.e. Lanzhou) should be improved. The different trend of CO and $NO_2$ may be partly due to the limited implementation of emission reduction measures in Lanzhou, as Lanzhou is an underdeveloping mega-city in the northwest of China with the lowest GDP among the 12 cities (see Table S1). In addition, the unique valley topography in Lanzhou is not conducive to the diffusion of air pollutants (Chen et al., 2020b), which may frequently offset the emission reduction efforts.

### 3.3.2 Second clean air action (2018-2020)

Continuing the efforts of first clean air action, the second clean air action (2018-2020) aimed to significantly reduce the total emission of major air pollutants, comparing with the base year of 2015 (Li et al., 2020). The concentrations and changes between 2015 to 2020 from 12 mega-cities before and after weather normalization are illustrated in Fig. S8. In addition, we also summarized the relative changes (%) of six criteria pollutants during 2015-2020 and 2018-2020 in Table 1.

From 2015 to 2020, 12 mega-cities have achieved significant reductions in observed $PM_{2.5}$ concentrations, ranging from 27% (Lanzhou) to 52% (Beijing) with an average of 39%. After the weather normalization, the reductions in deweathered $PM_{2.5}$ concentrations ranged from 20% to 43% (with an average of 36%). The reductions in deweathered $PM_{2.5}$ were significantly lower compared to the reduction in the observed $PM_{2.5}$ in Beijing, Shenzhen and Lanzhou, suggesting that meteorological conditions made a positive and significant contribution in enhancing reductions in $PM_{2.5}$ in these cities during time period of the second clean air action. By contrast, meteorological conditions made a negative contribution in $PM_{2.5}$ reduction at Shijiazhuang, as the magnitude of reduction increased after weather normalization.

Compared with the base year of 2015, all the 12 cities showed an obvious downward trend of observed $PM_{10}$ in 2020, and the reduction ranged from 27% (Guangzhou and Lanzhou) to 47% (Beijing). After the weather normalization, the magnitude of reduction ranged from 17% (Lanzhou) to 45% (Wuhan). The downward trends for $PM_{10}$ in Beijing, Shanghai, Nanjing, Shenzhen and Lanzhou were weakened greatly, indicating that meteorological conditions made a positive contribution in the control of $PM_{10}$ in these cities, amplifying the effect of emissions changes.

Among the 12 mega-cities, only Lanzhou showed an increase (0.6%) in observed $NO_2$ from 2015 to 2020, while the other 11 cities showed reductions with magnitudes ranging from 4.6% (Tianjin) to 39% (Beijing). After the weather normalization, the increase of $NO_2$ in Lanzhou was enlarged from 0.6% to 6.8%, indicating the inadequate effort of NOx reduction policies at this location. As shown in Fig. S8 and Table 1, compared to the observed concentrations, the reductions in deweathered $NO_2$ in Tianjin and Shanghai were enlarged greatly, suggesting a negative contribution of meteorological conditions in offsetting emission-change-driven NOx reductions in these cities.

All the 12 mega-cities showed an obvious decrease in $SO_2$ from 2015 to 2020, and the reductions of observed $SO_2$ ranged from 27% to 75%, with 9 cities (except Guangzhou, Shenzhen and Lanzhou) higher than 50%. The $SO_2$ reduction magnitudes in Beijing, Nanjing and Lanzhou were lowered greatly after the weather normalization, suggesting that the meteorological conditions made a positive contribution in amplifying the reduction of $SO_2$ in these cities.

8 cities (except Shanghai, Hangzhou, Shenzhen and Chengdu) showed an obvious increase of observed $O_3$ from 2015 to 2020, with the increase ranging from 6.6% to 39%. After weather normalization, only Hangzhou still showed a decrease in $O_3$ from 2015 to 2020, with magnitude change of only 1.4%. The downtrends in Shijiazhuang and Lanzhou were weakened, which means that meteorological conditions made a negative contribution in the suppressing reduction of $O_3$ in these cities. The performance of different cities varied widely when compared with the first clean

air action. It shows that some cities have made significant improvements in $O_3$ control during the second clean air action, while $O_3$ control is still a serious challenge for all these cities and further efforts are needed.

All the 12 cities showed obvious decrease in observed CO from 2015 to 2020, implying the remarkable emission reduction achieved through the second clean air action. The reductions of observed CO ranged from 19% (Hangzhou) to 50% (Beijing), with an average of 29%. By contrast, the reductions of deweathered CO ranged from 16% (Wuhan) to 43% (Beijing), with an average of 27%. The reductions of CO in Beijing, Lanzhou and Wuhan were weakened greatly after weather normalization, suggesting that meteorological conditions made a positive contribution in amplifying effects of the control of CO in these cities.

Here we also compare the overall reduction effectiveness from the average of 12 cities for both clean air actions, with the periods of 2013-2017 and 2018-2020. As shown in Table 1, both periods maintained similar reduction strength for $PM_{2.5}$, $PM_{10}$ and $SO_2$. Interestingly, it seems that the second clean air action made greater efforts in reducing NOx and CO, which may explain the slight decrease of observed $O_3$ during 2018-2020. This implies that the increasing trend severe $O_3$ pollution can be mitigated through continuous emission reduction.

We further summarize the difference between the observed and deweathered relative changes (from values shown in Table 1 and Fig. S8) for each city and six criteria pollutants. A positive value of these difference can indicate the negative contribution made by meteorological factors and vice versa. As shown in Table 1 and Fig. 3, a negative meteorological contribution was observed in most of the cities during the first clean air action, while most of the cities were tended to show a positive meteorological contribution during the second clean air action. However, the difference between the observed and deweathered relative changes are mostly below 5%, which suggests that the enhancement or reduction effect of meteorological are overall not significant for each city and six criteria pollutants. This demonstrates that the efforts from emission reduction remain the major driving force for the concentration changes of pollutants. We believe that these positive or negative contributions may be related to many factors, such as the periodic fluctuations in climate and the specific weather characteristics at each city, which still needs further investigation for more detailed explanation. Among the 12 mega-cites, only Beijing showed a positive meteorological contribution in reducing the main pollutants except $O_3$ during both the first and second clean air actions. This suggests that the improvement of air quality in Beijing was contributed from both emissions reductions of the two clean air actions and favorable meteorological conditions at the same period.

# 4.Conclusion

In this study, we employed the RF machine learning technique to decouple meteorological factors impacting ambient air quality data for 12 Chinese mega-cities during the period 2013-2020, in order to extract the real changes of air quality from large-scale emission reductions in recent years. With the exception of $O_3$, the observed concentrations of all the criteria pollutants showed significant reduction from 2013 to 2020, with an annual rate of decline for $PM_{2.5}$ in most cities of 6-8%, while $O_3$ showed an annual rate of increase of 1-9%. Compared with the observed results, all the pollutants showed smoothed but similar trends and rates of decline after weather normalization. We further quantify the extent to which these six criteria pollutants that are affected by meteorological conditions, and the results show that $PM_{2.5}$, $PM_{10}$, $SO_2$ and CO in Beijing are most sensitive to meteorology among the 12 mega-cities. By contrast, the responses of $NO_2$ and $O_3$ to meteorology did not show significant city-to-city difference. Significant regional differences of ozone formation chemistry were qualitatively determined through the fitted slopes in the $O_3$ vs. $NO_2$ spaces. Specifically, the $O_3$ formation in Pearl River Delta (PRD) region is more sensitive to NOx reduction, while $O_3$ formation in other regions is less sensitive to NOx reduction. The deweathered results emphasize the importance of VOC emission reductions in $O_3$ pollution mitigation in most cities if the meteorological influence is removed.

We further evaluate the effectiveness of first and second clean air actions by removing the meteorological influence. We find that both first and second clean air actions reduced most of the pollutants significantly, excepting the increase of $O_3$. However, meteorology can play negative or positive role by suppressing or amplifying changes due to emission controls respectively, which ranges from -9% to 16% depending on specific conditions, such as the type of pollutants, locations, and time period. For example, a negative meteorological contribution was observed in most of the cities during the first clean air action, while most of the cities were tended to show a positive meteorological contribution during the second clean air action. Among the 12 mega-cites, only Beijing showed a positive meteorological contribution in reducing the main pollutants except $O_3$ during both the first and second clean air actions. Considering the significant scope for meteorological effects to change air quality, and obscure the effectiveness of policy actions, we suggest that such deweathered analyses are routinely undertaken on a regional basis.

## Conflicts of interest

The authors declare that they have no conflicts of interest.

## Acknowledgement

We thank Tuan V. Vu and Zongbo Shi from University of Birmingham for distributing the RF model code.

## CRediT authorship contribution statement

**Yong Guo**: Formal analysis, Investigation, Software, Visualization, Writing- Original draft preparation; **Kangwei Li**: Conceptualization, Supervision, Resources, Writing- Reviewing and Editing; **Bin Zhao**: Investigation, Writing- Reviewing and Editing; **Jiandong Shen**: Resources; **William J. Bloss**: Investigation, Writing- Reviewing and Editing; **Merched Azzi**: Writing- Reviewing and Editing; **Yinping Zhang**: Resources, Writing- Reviewing and Editing.

## References

Blanchard CL. Ozone process insights from field experiments – Part III: extent of reaction and ozone formation. Atmospheric Environment 2000; 34: 2035-2043.

Chen L, Zhu J, Liao H, Yang Y, Yue X. Meteorological influences on PM2.5 and O3 trends and associated health burden since China's clean air actions. Sci Total Environ 2020a; 744: 140837.

Chen T, Li Z, Zhou X, Wang F, Zhang X, Wang F. Air pollution characteristics,source analysis and cause of formation under the background ofLanzhou blue. Acta Scientiae Circumstantiae 2020b; 40: 1361-1373.

Chen Z, Wang J-N, Ma G-X, Zhang Y-S. China tackles the health effects of air pollution. The Lancet 2013; 382: 1959-1960.

Cui XL, Wei XQ, Wang T, Iop. Research progress of extreme climate and its vegetation response. 2nd International Conference on Materials Science, Energy Technology and Environmental Engineering. 81, 2017.

Daskalakis N, Tsigaridis K, Myriokefalitakis S, Fanourgakis GS, Kanakidou M. Large gain in air quality compared to an alternative anthropogenic emissions scenario. Atmos. Chem. Phys. 2016; 16: 9771-9784.

Ding AJ, Fu CB, Yang XQ, Sun JN, Zheng LF, Xie YN, et al. Ozone and fine particle in the western Yangtze River Delta: an overview of 1 yr data at the SORPES station. Atmos. Chem. Phys. 2013; 13: 5813-5830.

Emery C, Liu Z, Russell AG, Odman MT, Yarwood G, Kumar N. Recommendations on statistics and benchmarks to assess photochemical model performance. Journal of the Air & Waste Management Association 2017; 67: 582-598.

Fan H, Zhao C, Yang Y. A comprehensive analysis of the spatio-temporal variation of urban air pollution in China during 2014–2018. Atmospheric Environment 2020; 220.

Feng L, Ye B, Feng H, Ren F, Huang S, Zhang X, et al. Spatiotemporal Changes in Fine Particulate Matter Pollution and the Associated Mortality Burden in China between 2015 and 2016. Int J Environ Res Public Health 2017; 14.

Gao M, Han Z, Liu Z, Li M, Xin J, Tao Z, et al. Air quality and climate change, Topic 3 of the Model Inter-Comparison Study for Asia Phase III (MICS-Asia III) – Part 1: Overview and model evaluation. Atmos. Chem. Phys. 2018; 18: 4859-4884.

Grange SK, Carslaw DC. Using meteorological normalisation to detect interventions in air quality time series. Sci Total Environ 2019; 653: 578-588.

Grange SK, Carslaw DC, Lewis AC, Boleti E, Hueglin C. Random forest meteorological normalisation models for Swiss PM10 trend analysis. Atmos. Chem. Phys. 2018; 18: 6223-6239.

Guo P, Umarova AB, Luan Y. The spatiotemporal characteristics of the air pollutants in China from 2015 to 2019. PLoS One 2020; 15: e0227469.

Hadley MB, Vedanthan R, Fuster V. Air pollution and cardiovascular disease: a window of opportunity. Nat Rev Cardiol 2018; 15: 193-194.

He G, Pan Y, Tanaka T. The short-term impacts of COVID-19 lockdown on urban air pollution in China. Nature Sustainability 2020; 3.

Henneman LRF, Holmes HA, Mulholland JA, Russell AG. Meteorological detrending of primary and secondary pollutant concentrations: Method application and evaluation using long-term (2000–2012) data in Atlanta. Atmospheric Environment 2015; 119: 201-210.

Herrera-Estrada JE, Diffenbaugh NS, Wagner F, Craft A, Sheffield J. Response of electricity sector air pollution emissions to drought conditions in the western United States. Environmental Research Letters 2018; 13.

Hidy GM. Ozone process insights from field experiments – part I: overview. Atmospheric Environment

2000; 34: 2001-2022.
Hu J, Ying Q, Wang Y, Zhang H. Characterizing multi-pollutant air pollution in China: Comparison of three air quality indices. Environ Int 2015; 84: 17-25.
Kuerban M, Waili Y, Fan F, Liu Y, Qin W, Dore AJ, et al. Spatio-temporal patterns of air pollution in China from 2015 to 2018 and implications for health risks. Environ Pollut 2020; 258: 113659.
Li D, Liu J, Zhang J, Gui H, Du P, Yu T, et al. Identification of long-range transport pathways and potential sources of PM2.5 and PM10 in Beijing from 2014 to 2015. J Environ Sci (China) 2017; 56: 214-229.
Li K, Jacob DJ, Liao H, Shen L, Zhang Q, Bates KH. Anthropogenic drivers of 2013–2017 trends in summer surface ozone in China. Proceedings of the National Academy of Sciences 2019; 116: 422.
Li R, Xu M, Li M, Chen Z, Zhao N, Gao B, et al. Identifying the spatiotemporal variations in ozone formation regimes across China from 2005 to 2019 based on polynomial simulation and causality analysis. Atmos. Chem. Phys. 2021; 21: 15631-15646.
Li W, Shao L, Wang W, Li H, Wang X, Li Y, et al. Air quality improvement in response to intensified control strategies in Beijing during 2013-2019. Sci Total Environ 2020; 744: 140776.
Liang P, Zhu T, Fang Y, Li Y, Han Y, Wu Y, et al. The role of meteorological conditions and pollution control strategies in reducing air pollution in Beijing during APEC 2014 and Victory Parade 2015. Atmospheric Chemistry and Physics 2017; 17: 13921-13940.
Lin C, Lau AKH, Fung JCH, Song Y, Li Y, Tao M, et al. Removing the effects of meteorological factors on changes in nitrogen dioxide and ozone concentrations in China from 2013 to 2020. Sci Total Environ 2021; 793: 148575.
Liu Y, Wang T. Worsening urban ozone pollution in China from 2013 to 2017 – Part 1: The complex and varying roles of meteorology. Atmospheric Chemistry and Physics 2020; 20: 6305-6321.
Lu X, Hong J, Zhang L, Cooper OR, Schultz MG, Xu X, et al. Severe Surface Ozone Pollution in China: A Global Perspective. Environmental Science & Technology Letters 2018; 5: 487-494.
Ma T, Duan F, He K, Qin Y, Tong D, Geng G, et al. Air pollution characteristics and their relationship with emissions and meteorology in the Yangtze River Delta region during 2014-2016. J Environ Sci (China) 2019; 83: 8-20.
Meng K, Xu X, Cheng X, Xu X, Qu X, Zhu W, et al. Spatio-temporal variations in SO2 and NO2 emissions caused by heating over the Beijing-Tianjin-Hebei Region constrained by an adaptive nudging method with OMI data. Sci Total Environ 2018; 642: 543-552.
Shi ZB, Song CB, Liu BW, Lu GD, Xu JS, Vu TV, et al. Abrupt but smaller than expected changes in surface air quality attributable to COVID-19 lockdowns. Science Advances 2021; 7.
Song C, Ma C, Zhang Y, Wang T, Wu L, Wang P, et al. Heavy-duty diesel vehicles dominate vehicle emissions in a tunnel study in northern China. SCIENCE OF THE TOTAL ENVIRONMENT 2018; 637: 431-442.
Song C, Wu L, Xie Y, He J, Chen X, Wang T, et al. Air pollution in China: Status and spatiotemporal variations. Environ Pollut 2017; 227: 334-347.
Sun L, Xue L, Wang Y, Li L, Lin J, Ni R, et al. Impacts of meteorology and emissions on summertime surface ozone increases over central eastern China between 2003 and 2015. Atmos. Chem. Phys. 2019; 19: 1455-1469.
Tie X, Huang R-J, Dai W, Cao J, Long X, Su X, et al. Effect of heavy haze and aerosol pollution on rice and wheat productions in China. Scientific Reports 2016; 6.

Venter ZS, Aunan K, Chowdhury S, Lelieveld J. COVID-19 lockdowns cause global air pollution declines. Proceedings of the National Academy of Sciences of the United States of America 2020; 117: 18984-18990.

Vu TV, Shi Z, Cheng J, Zhang Q, He K, Wang S, et al. Assessing the impact of clean air action on air quality trends in Beijing using a machine learning technique. Atmospheric Chemistry and Physics 2019; 19: 11303-11314.

Wang L, Xiong Q, Wu G, Gautam A, Jiang J, Liu S, et al. Spatio-Temporal Variation Characteristics of PM2.5 in the Beijing–Tianjin–Hebei Region, China, from 2013 to 2018. International Journal of Environmental Research and Public Health 2019a; 16.

Wang N, Lyu X, Deng X, Huang X, Jiang F, Ding A. Aggravating O3 pollution due to NOx emission control in eastern China. Science of The Total Environment 2019b; 677: 732-744.

Wang R, Asghari V, Hsu S-C, Lee C-J, Chen J-H. Detecting corporate misconduct through random forest in China's construction industry. Journal of Cleaner Production 2020a; 268: 122266.

Wang S, Huang G, Lin JT, Hu KM, Wang L, Gong HN. Chinese blue days: a novel index and spatio-temporal variations. Environmental Research Letters 2019c; 14.

Wang X, Sun W, Zheng K, Ren X, Han P. Estimating hourly PM2.5 concentrations using MODIS 3 km AOD and an improved spatiotemporal model over Beijing-Tianjin-Hebei, China. Atmospheric Environment 2020b; 222.

Xiao Q, Zheng Y, Geng G, Chen C, Huang X, Che H, et al. Separating emission and meteorological contributions to long-term PM<sub>2.5</sub> trends over eastern China during 2000–2018. Atmospheric Chemistry and Physics 2021; 21: 9475-9496.

Xu M, Qin Z, Zhang S. Carbon dioxide mitigation co-effect analysis of clean air policies: lessons and perspectives in China's Beijing-Tianjin-Hebei region. Environmental Research Letters 2021; 16.

Zhan Y, Luo Y, Deng X, Grieneisen ML, Zhang M, Di B. Spatiotemporal prediction of daily ambient ozone levels across China using random forest for human exposure assessment. Environ Pollut 2018; 233: 464-473.

Zhang H, Wang Y, Hu J, Ying Q, Hu XM. Relationships between meteorological parameters and criteria air pollutants in three megacities in China. Environ Res 2015; 140: 242-54.

Zhang NN, Ma F, Qin CB, Li YF. Spatiotemporal trends in PM2.5 levels from 2013 to 2017 and regional demarcations for joint prevention and control of atmospheric pollution in China. Chemosphere 2018; 210: 1176-1184.

Zhang Q, Zheng Y, Tong D, Shao M, Wang S, Zhang Y, et al. Drivers of improved PM2.5 air quality in China from 2013 to 2017. Proc Natl Acad Sci U S A 2019; 116: 24463-24469.

Zhang Y, Vu TV, Sun J, He J, Shen X, Lin W, et al. Significant Changes in Chemistry of Fine Particles in Wintertime Beijing from 2007 to 2017: Impact of Clean Air Actions. Environ Sci Technol 2020; 54: 1344-1352.

Zheng B, Tong D, Li M, Liu F, Hong C, Geng G, et al. Trends in China's anthropogenic emissions since 2010 as the consequence of clean air actions. Atmospheric Chemistry and Physics 2018; 18: 14095-14111.

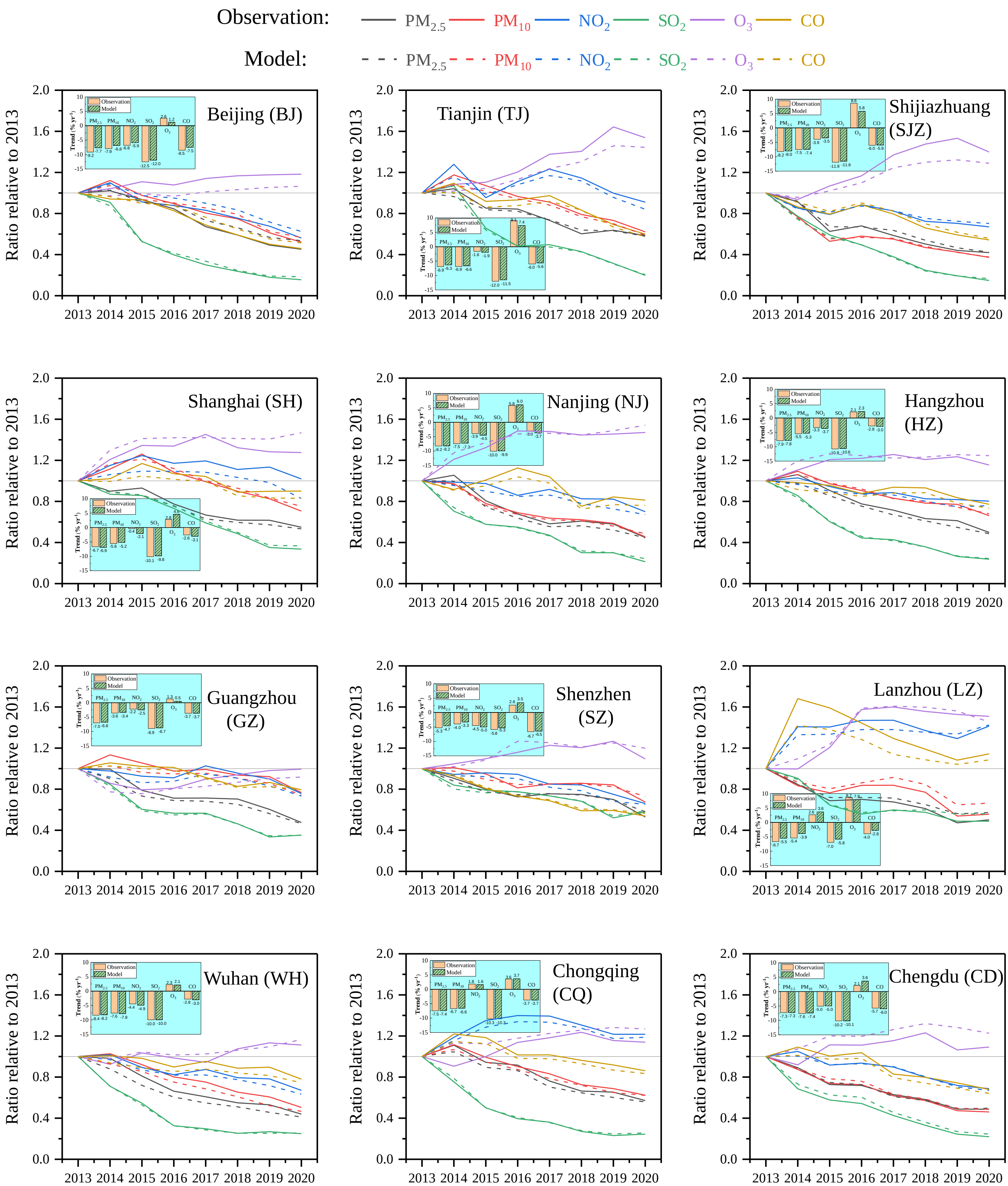


**Figure. 1** The normalized trend (observed and RF modelled) of the six criteria pollutants in the 12 mega-cities from 2013 to 2020. Inserts show the overall mean annual change rates from 2013-2020.

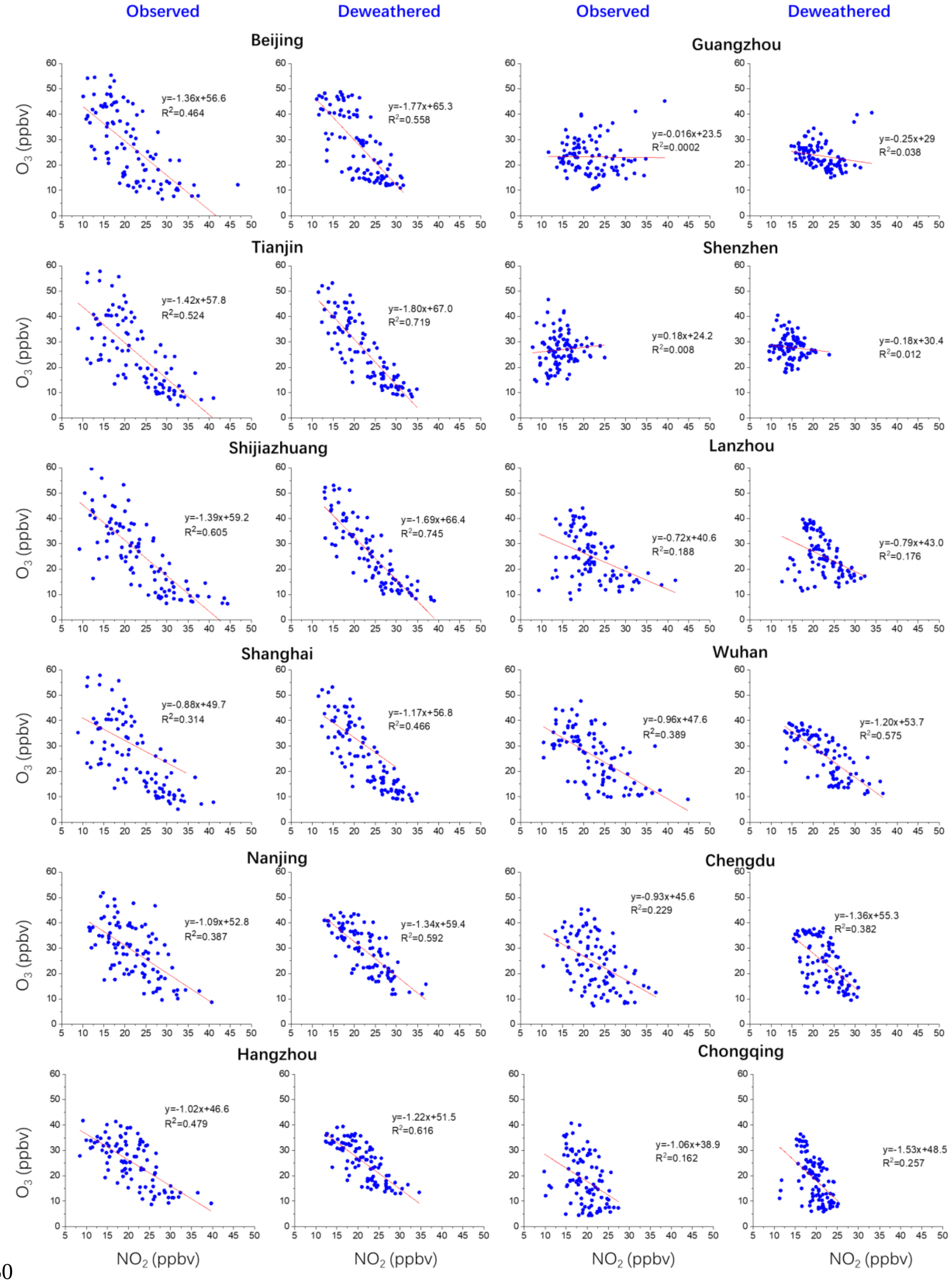


**Figure. 2** The monthly averaged $O_3$ vs. $NO_2$ (observed and RF modelled) from 96 months between 2013 to 2020 for 12 mega-cities

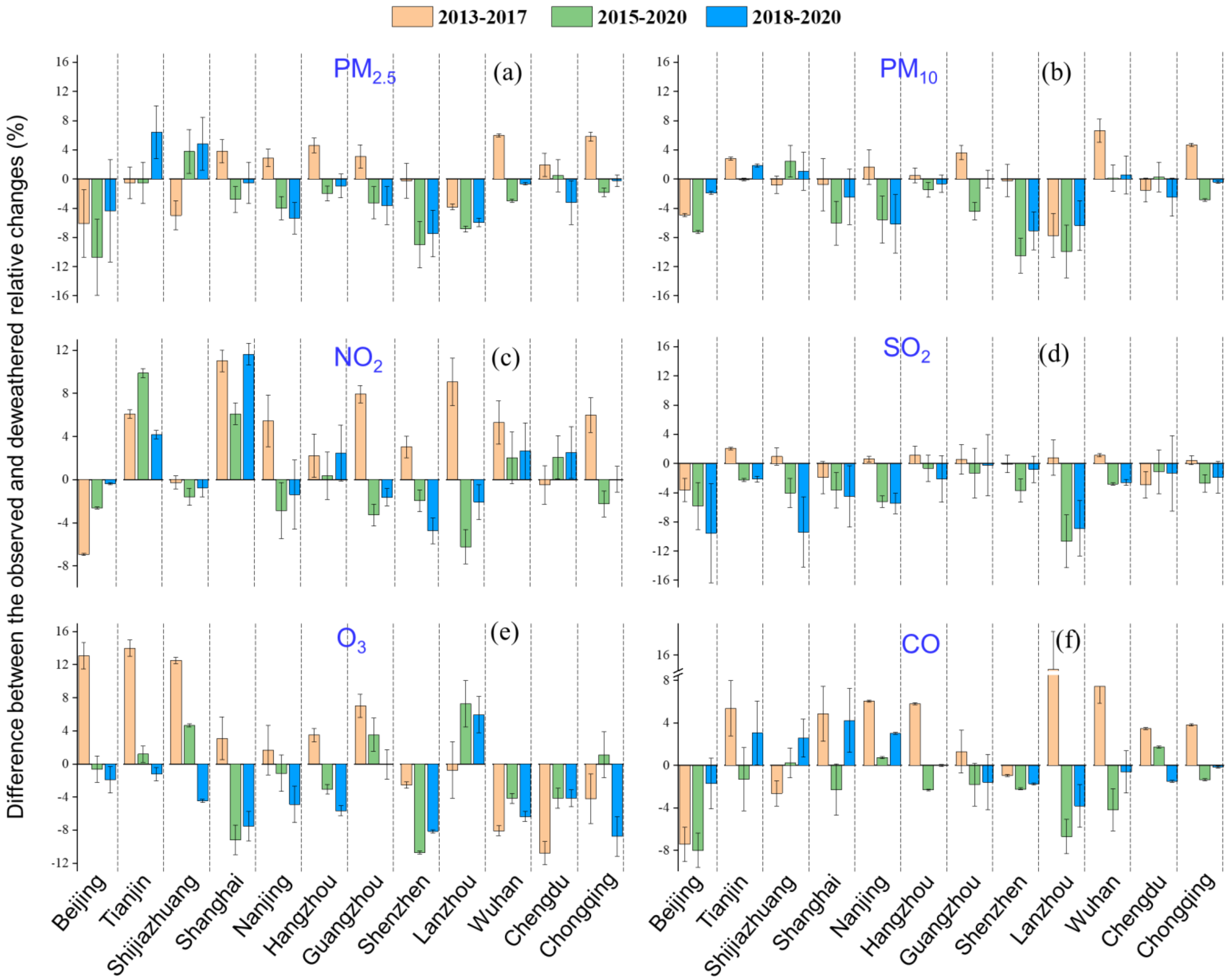


**Figure. 3** The difference between the observed and deweathered relative changes (as shown in Figure S8) of the six criteria pollutants in 12 mega-cities. The statistic metric mean bias (MB) in Table S3 was employed as the uncertainty error of RF model.

**Table 1.** The relative changes (%) of six criteria pollutants from 2013 to 2017, 2015 to 2020, and 2018 to 2020 in 12 mega-cities.

| | | **Observed concentration** | | | | | | **Deweathered concentration** | | | | | |
|---|---|---|---|---|---|---|---|---|---|---|---|---|---|
| | | $PM_{2.5}$ | $PM_{10}$ | $NO_2$ | $SO_2$ | $O_3$ | CO | $PM_{2.5}$ | $PM_{10}$ | $NO_2$ | $SO_2$ | $O_3$ | CO |
| **Beijing** | 2013-2017 | -33 | -20 | -17 | -70 | 14 | -31 | -27 | -15 | -10 | -66 | 1 | -24 |
| | 2015-2020 | -52 | -47 | -39 | -71 | 6.6 | -50 | -41 | -39 | -36 | -65 | 7.2 | -43 |
| | 2018-2020 | -23 | -30 | -26 | -35 | 1.3 | -22 | -19 | -28 | -25 | -25 | 3.2 | -21 |
| **Tianjin** | 2013-2017 | -27 | -8.9 | 23 | -60 | 37 | -2.6 | -26 | -12 | 17 | -52 | 24 | -8 |
| | 2015-2020 | -31 | -42 | -4.6 | -70 | 39 | -34 | -31 | -42 | -15 | -68 | 38 | -34 |
| | 2018-2020 | -3 | -21 | -21 | -54 | 9.5 | -28 | -9.4 | -23 | -25 | -52 | 11 | -31 |
| **Shijiazhuang** | 2013-2017 | -41 | -45 | -18 | -62 | 37 | -20 | -36 | -44 | -17 | -63 | 24 | -18 |
| | 2015-2020 | -33 | -30 | -15 | -75 | 31 | -32 | -37 | -32 | -14 | -71 | 26 | -32 |
| | 2018-2020 | -17 | -21 | -7.4 | -40 | -5.2 | -18 | -21 | -22 | -6.6 | -31 | -0.8 | -20 |
| **Shanghai** | 2013-2017 | -33 | -0.8 | 19 | -41 | 45 | 4.3 | -37 | -0.02 | 8.4 | -30 | 42 | -0.6 |
| | 2015-2020 | -41 | -44 | -18 | -61 | -5.1 | -23 | -38 | -38 | -24 | -57 | 4 | -21 |
| | 2018-2020 | -11 | -21 | -8.3 | -31 | -3.5 | 1.3 | -11 | -19 | -20 | -26 | 4 | -2.9 |
| **Nanjing** | 2013-2017 | -42 | -36 | -8.2 | -53 | 48 | 4 | -45 | -38 | -14 | -54 | 46 | -2.1 |
| | 2015-2020 | -44 | -42 | -28 | -63 | 11 | -20 | -40 | -36 | -25 | -58 | 12 | -20 |
| | 2018-2020 | -26 | -27 | -15 | -29 | 1.7 | 7.8 | -21 | -21 | -14 | -24 | 6.6 | 4.7 |
| **Hangzhou** | 2013-2017 | -28 | -17 | -11 | -57 | 26 | -6.2 | -33 | -17 | -14 | -58 | 22 | -12 |
| | 2015-2020 | -45 | -32 | -15 | -61 | -4.4 | -19 | -43 | -31 | -15 | -60 | -1.4 | -17 |
| | 2018-2020 | -21 | -16 | -2.8 | -34 | -4.5 | -17 | -20 | -15 | -5.2 | -32 | 1.2 | -17 |
| **Guangzhou** | 2013-2017 | -29 | -0.8 | 2.7 | -43 | -10 | -8.7 | -32 | -4.4 | -5.3 | -44 | -17 | -10 |
| | 2015-2020 | -40 | -27 | -18 | -42 | 25 | -22 | -36 | -23 | -15 | -40 | 22 | -20 |
| | 2018-2020 | -32 | -18 | -21 | -24 | 5.8 | -4.1 | -29 | -18 | -19 | -24 | 5.8 | -2.5 |
| **Shenzhen** | 2013-2017 | -25 | -15 | -15 | -27 | 23 | -31 | -24 | -15 | -18 | -26 | 25 | -30 |
| | 2015-2020 | -34 | -29 | -31 | -27 | -0.1 | -33 | -25 | -18 | -29 | -23 | 11 | -31 |
| | 2018-2020 | -29 | -21 | -22 | -15 | -9.1 | -8.8 | -22 | -14 | -17 | -14 | -1 | -7 |
| **Lanzhou** | 2013-2017 | -32 | -16 | 47 | -40 | 60 | 29 | -29 | -8.5 | 38 | -41 | 61 | 14 |
| | 2015-2020 | -27 | -27 | 0.6 | -24 | 25 | -28 | -20 | -17 | 6.8 | -14 | 18 | -21 |
| | 2018-2020 | -18 | -28 | 3.2 | -15 | -3.1 | -3.8 | -12 | -21 | 5.3 | -6.2 | -9 | 0 |
| **Wuhan** | 2013-2017 | -39 | -25 | -13 | -70 | -5.6 | -4.7 | -45 | -31 | -18 | -71 | 2.4 | -12 |
| | 2015-2020 | -46 | -45 | -25 | -54 | 7.4 | -21 | -43 | -45 | -27 | -52 | 12 | -16 |
| | 2018-2020 | -20 | -23 | -16 | -1.6 | 3.5 | -12 | -19 | -23 | -18 | 1 | 9.8 | -11 |
| **Chengdu** | 2013-2017 | -37 | -38 | -10 | -57 | 15 | -17 | -39 | -37 | -9.7 | -54 | 26 | -21 |
| | 2015-2020 | -33 | -38 | -25 | -62 | -1.9 | -32 | -34 | -38 | -27 | -61 | 2.2 | -34 |
| | 2018-2020 | -16 | -19 | -14 | -34 | -11 | -15 | -13 | -17 | -17 | -32 | -7.1 | -13 |
| **Chongqing** | 2013-2017 | -24 | -17 | 39 | -64 | 18 | 1.6 | -30 | -22 | 32 | -64 | 22 | -2.2 |
| | 2015-2020 | -39 | -37 | -10 | -51 | 14 | -27 | 38 | -34 | -7.7 | -48 | 13 | -26 |
| | 2018-2020 | -14 | -14 | -6.9 | -9.6 | -7.8 | -11 | -14 | -14 | -6.9 | -7.7 | 1 | -10 |
| **Average in 12 cities** | 2013-2017 | -34 | -25 | 0 | -56 | 24 | -9 | -34 | -25 | -3.4 | -56 | 21 | -11 |
| | 2015-2020 | -39 | -37 | -19 | -59 | 11 | -29 | -36 | -34 | -19 | -55 | 13 | -27 |
| | 2018-2020 | -19 | -22 | -13 | -29 | -1.9 | -12 | -17 | -20 | -14 | -25 | 2.1 | -12 |